Microfabrication of Capillary Electrospray Emitters and ToF Characterization of the Emitted Beam

IEPC-2011-131

Presented at the 32nd International Electric Propulsion Conference,
Wiesbaden • Germany
September 11 – 15, 2011

S. Dandavino[1], C. Ataman[2] and H. Shea[3]
École Polytechnique Fédérale de Lausanne (EPFL), Neuchatel, 2000, Switzerland

C. Ryan[4] and J. Stark[5]
Queen Mary University of London, London, E1 4NS, United Kingdom

Abstract: Microfabrication, assembly, and characterization of internally fed arrays of electrospray emitters for spacecraft propulsion are discussed. Several different emitter geometries were fabricated, and the sprayed beams from these emitters are characterized for their ion/droplet composition. It is shown that with smaller inner diameters, ionic mode of operation can be achieved more easily, due to the increase in the hydraulic impedance. Up to 2000 s I_{sp} was measured from capillaries with 5 µm inner diameter and 100 µm with 750V extraction voltage using EMI-BF_4. Due to the small dimensions of the microfabricated capillaries, the onset and ionic mode operation voltages can be significantly lower than macroscopic emitters. The major failure mode for the emitters was the liquid overflow from the capillary tip, which can be resolved through coatings that wet the ionic liquids differently. A detailed study of the wetting behavior of two ionic liquids is also presented for various materials compatible with silicon microfabrication technology.

Nomenclature

DRIE	=	Deep Reactive Ion Etch
EMI-BF_4	=	1- ethyl-3-methylimidazolium tetrafluoroborate
EMI-TF_2N	=	1- ethyl-3-methylimidazolium bis(trifluoromethylsulfonyl)imid
IL	=	Ionic Liquid
I_{sp}	=	Specific Impulse
MVD	=	Molecular Vapor Deposition
SOI	=	Silicon-On-Insulator
ToF	=	Time of Flight
TRL	=	Technology Readiness Level

[1] PhD Student, Microsystems for Space Technologies Laboratory (IMT - LMTS), simon.dandavino@epfl.ch
[2] Post-doc, Microsystems for Space Technologies Laboratory (IMT - LMTS), caglar.ataman@epfl.ch
[3] Associate Professor, Microsystems for Space Technologies Laboratory (IMT - LMTS), herbert.shea@epfl.ch
[4] Post-doc, School of Engineering and Materials Science, c.n.ryan@qmul.ac.uk
[5] Professor, School of Engineering and Materials Science, j.p.w.stark@qmul.ac.uk

I. Introduction

MICROFABRICATED electrospray ion sources are a promising technology for providing high delta-V propulsion capabilities for small (<100 kg) spacecraft. They typically operate by transporting ionic liquid (IL) to an annular electrode placed above an extraction site. As the potential between the conductive IL and the electrode is increased, the IL deforms into a Taylor cone[1] and eventually starts spraying droplets or, if the dimensions, IL properties, and applied field are adequate, single ions[2]. Transporting the IL through capillary action further removes the need for active pumping and provides significant reductions in system complexity. Demonstrated electrosprays using capillary transport of propellant can be separated in three types: externally wetted[3], wetted through porous materials[4,5] or internally wetted[6,7].

Our group has focused on the last method, using microfabricated arrays of silicon capillaries aligned under an array of microfabricated extraction electrodes. Previously published results[8] described how the operation mode of the thrusters could be tailored from droplet to ion mode with the use of silica microbeads that increased the hydraulic impedance of the 18-32 µm inner diameter capillaries. High hydraulic impedance also reduced the occurrence of ionic liquid overflow that caused device failure.

Our current efforts are to achieve this high impedance without bead filling through further miniaturization. Wafer level integration of the extractor electrode was also introduced, simplifying the assembly process. Fabricated devices were successfully tested with IV and Time of Flight (ToF) curves traced. In an effort to understand and eventually limit IL overflow, sessile drop tests were also performed to evaluate the contact angle in vacuum of EMI-BF_4 and EMI-TF_2N with several substrates. This work is carried out in the framework of the MicroThrust project[6] which aims to develop to Technology Readiness Level (TRL-5) a system based on this technology.

II. Thruster Design

The thruster consists of an emitter and an extractor integrated with a 50 µm thick polymer layer in between. A cross section of the assembly is shown in Figure 1. The capillaries stand off the silicon surface and each face an individual annular extractor electrode. The intention of this layout is to guarantee homogeneous spray characteristics across the array. The extractor electrode chip is electrically isolated from the capillary one by the said polymer layer. The capillary tip is etched to enhance the sharpness of the tip and reduce the total tip area, should the liquid wet the entire top surface.

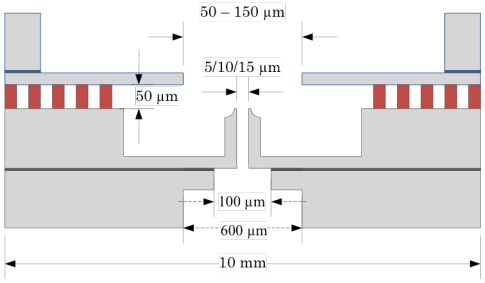

Figure 1. Cross-section view of the integrated thruster module. Please note that the drawing is not to proportions.

III. Fabrication

Microfabrication offers unmatched precision compared to other conventional machining methods, and enables the batch manufacturing of precision structures with features in the micrometer range. Within the context of an electrospray thruster, the most important advantage of using microfabricated emitters is the possibility of packing many emitters within a small area and therefore boosting the thrust density, a fundamental limitation for such thrusters. In this work, the two basics components of an electrospray thruster, namely the capillary emitter and the extractor electrode are fabricated on separate wafers then integrated through a wafer bonding process. Therefore, the major task of assembly with good capillary-extractor alignment (within a few microns) is accomplished without manual intervention. Below are the fabrication details for the micromachining and wafer bonding steps.

A. Emitter & extractor fabrication

The fabrication of the emitters and the extractors are based on silicon-on-insulator (SOI) wafers from a commercial supplier. These wafers consist of a thin silicon oxide (SiO_2) layer sandwiched between two thicker single-crystal silicon layers. As a stopping layer during silicon etching, this buried oxide enables very good height

[6] www.microthrust.net

control for the structures machined on both sides of the wafer. For both the capillaries and the emitters, the process begins with thermal oxidation (2.2 µm). The first lithography, wet oxide etch and the consecutive Deep Reactive Ion Etch (DRIE) defines the extractors on the device layer of the extractor wafer, which has 50/2/400 µm thick device/oxide/handle layers (Figure 2b). The extractor dimensions vary from 75 µm to 200 µm. A similar set of steps follow for the opening of the extractors from the backside. The thick handle layer acts both as a support layer for the relatively thin extractors and also as a spacer with well-defined thickness between the extractors and a possible integrated accelerator electrode. Finally, the buried oxide and the remaining oxide layers on both faces are removed and the wafers are coated with 200 nm of aluminum on both sides to maintain uniform potential distribution all along the extractor chip (Figure 2c).

Figure 2: Fabrication steps for the extractor wafers. The SOI wafers have 50 µm thick device layer, 2 µm thick buried.

The process for the capillaries is more involved with several more etching and lithography steps. Via the first lithography/wet oxide etch/DRIE sequence the 100 µm deep capillaries are defined on the device layer. This etch constitutes the most critical step within the process flow due to the very high aspect ratio required (Figure 3b). The optimization of the etch parameters is of utmost importance to ensure small capillaries with high hydraulic

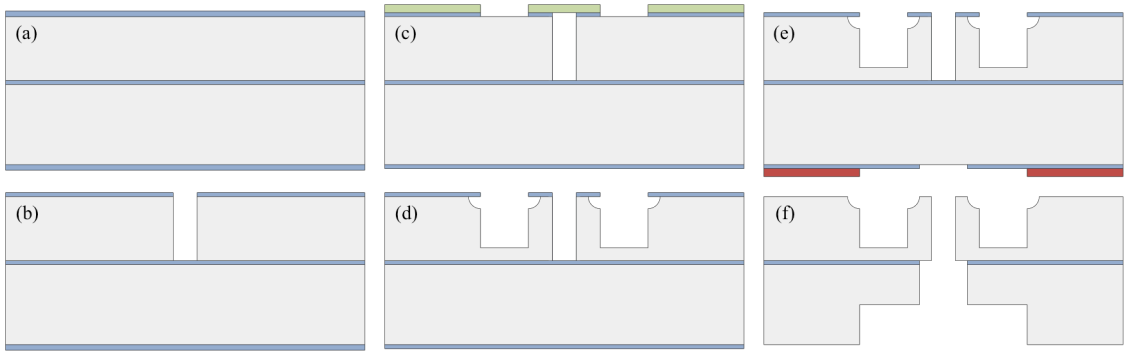

Figure 3: Fabrication steps for the extractor wafers. The SOI wafers have 100 µm thick device layer, 2 µm thick buried oxide layer, and 500 µm thick handle layer. The thermal oxide on both faces is 2.2 µm thick.

impedance. There are three different capillary designs: 5, 10, and 15 µm inner diameters. For the lithography defining the outer capillary walls, DuPont MX5015[7] laminated dry photoresist is used, since it provides good coverage over the structured surface (Figure 3c). The emitters are then shaped by an isotropic silicon etch (to increase tip sharpness) and a consecutive DRIE step (Figure 3d). The capillary fabrication is completed by the definition of a backside reservoir via a two layer etch (Figure 3f). A stacked photoresist and oxide mask is used for this last backside etch, which is followed by the release of the chips in a wet oxide etching bath.

B. Wafer level bonding

The impact of wafer bonding technologies on microelectronics and MEMS has been substantial. They enabled these predominantly planar machining methods to extend vertically and explore the possibilities of complex 3D structures. The recent drastic increase of the academic and industrial interest in wafer bonding has led to the development of a wide spectrum of bonding methods, including anodic (silicon/glass), fusion (silicon/silicon), eutectic (silicon/metal), and polymer bonding. The choice of the bonding method depends heavily on the nature of the substrates to be bonded, and the application of the device. For the integration of the capillary and extractor wafers described in the previous subsection, the bonding interface should be electrically isolating with enough dielectric strength to withstand high potential differences between the surfaces, implemented in different thicknesses for design flexibility and geometry optimization, and if possible, detachable to enable inspection of the surfaces

[7] http://www2.dupont.com/WLP/en_US/assets/downloads/pdf/MX5000.pdf

post-testing. To meet the above requirements, a new bonding method using DuPont MX5000 series laminated dry photoresists was developed. This SU8 based resist film, developed for thick electroplating processes, is offered in various thicknesses and has a dielectric strength of 120 kV/mm. A film of 50 µm thickness can therefore withstand a potential difference of 6 kV, which is significantly larger than the voltages involved in the operation of our devices.

Fundamental steps of the bonding and singulation process are illustrated in Figure 4. The extractor wafer was chosen as the carrier surface for the bonding polymer. The dry photo resist film is laminated using a semi-automatic lamination tool with roll temperature of 85°C, roll pressure of 2 bars, and roll speed of 1.2 m/min. Post-lamination bake, which enhances the resist adhesion, is avoided. Patterning of the resist is the same as conventional photoresists with an exposure intensity of 110 mJ/cm^2. Alignment of the two wafers prior to the bonding is of utmost importance. A Karl Süss BA6 type bond alignment tool is used for alignment and pre-bonding (5 min @ 125°C with no applied pressure). The actual bonding follows the alignment and is performed with a manual bonding tool under 115 °C and 92 N/cm^2 pressure. After 1 hour, the temperature is gradually decreased down to 50 °C over 45 minutes. After bonding, the stack is sandwich between two dicing tapes to prevent sample contamination during the mechanical dicing step, by which the wafers are singulated into 1 cm by 1 cm thruster chips. The non-permanent (the bonding resist can chemically be removed even after the curing process) wafer level assembly of the emitters and extractor allows the disassembly of the thruster for failure analysis and can provide better than 5 µm alignment. An SEM image of an integrated thruster array is shown in Figure 5.

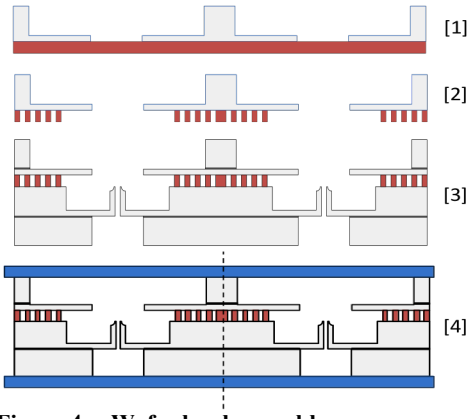

Figure 4: Wafer level assembly process

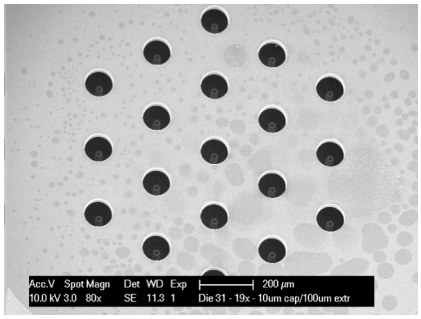

Figure 5: SEM picture of an integrated thruster array. The emitter inner diameter is 10 µm, and the extractors are 100 µm.

IV. Thruster Characterization

A. Experimental setup

The characterization of the thruster modules is performed at QMUL with a time-of-flight system. A layout of the setup is given in Figure 6. The test bench consists of a vacuum chamber for thrust performance characterization and a second chamber for test liquid storage. The storage of ionic liquid in the absence of background water vapor and other contaminants also enables the degassing of the ionic liquid before filling the thruster. This approach avoids bubble formation during thruster filling. Both chambers are connected through a silica capillary tube to transfer the liquid from the reservoir to the thruster. The base pressure attained in the main chamber is below 1×10^{-6} mbar and in the fluid reservoir below 1.3×10^{-3} mbar. For spray testing the emitter capillaries are connected to a high voltage source. During all tests the extractor electrodes are grounded and the emitter capillaries biased to high voltage. The electrospray current is measured by means of a Faraday cup (Kimball Physics FC-72A, which is located at the end of the 40 cm long time-of-flight tube. The output of the Faraday cup is first amplified from the nano-ampere range using a variable-gain high-speed current amplifier (Laser Instruments, model DHCPA-100) with a gain of 10^7 V/A at 1.6 MHz bandwidth.

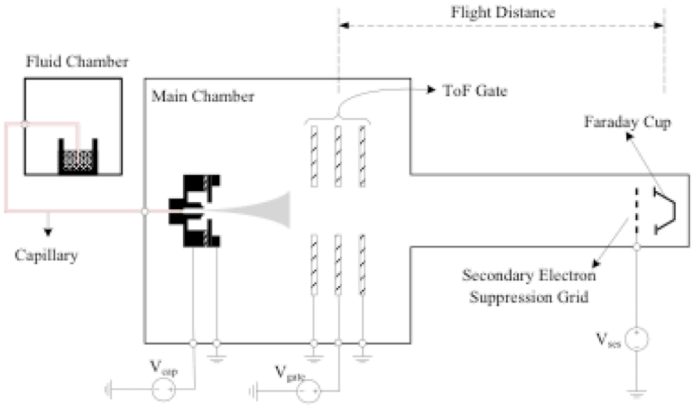

Figure 6: Schematic drawing of the time-of-flight system used for thruster characterization.

This signal was measured by a digital storage oscilloscope (Wavetek, Wavesurfer 422) through 50 Ω dc coupling at 20 MHz bandwidth.

B. Test assembly

The thruster modules are placed into the test chamber with a simple assembly that provides the electrical and fluidic interfaces to the module. A schematic drawing of this assembly is depicted in Figure 7a. For the containment of the liquid, a simple EPDM rubber O-ring is used between the thruster module and the aluminum chip holder providing a tight seal when the thruster module is fastened in place by a laser machined steel plate. This steel plate is in contact with the extractor electrode, providing the first electrical lead. The liquid is addressed through the aluminum chip holder.

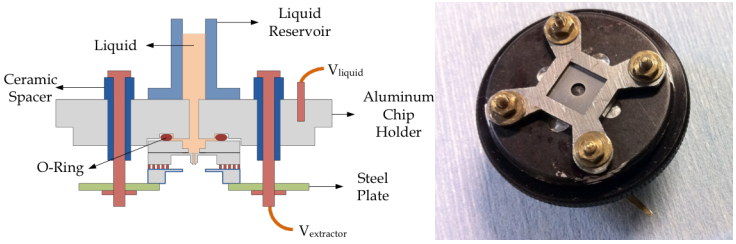

Figure 7: (a) Schematics of the test assembly. (b) A photograph of the assembly.

C. Results

Figure 8 illustrates a typical TOF curve of the beam spray from a 10 µm diameter capillary using EMI-BF_4 as the liquid. The test was carried out in unipolar mode, with a 10μm emitter at a potential difference of +750V. The applied back pressure was 1.3×10^{-3} mBar; i.e. the reservoir chamber was completely evacuated. This lack of, or only small, back pressure was found to be necessary for the 10 and 15µm chips, as greater applied pressures resulted in the liquid bridging between the emitter and the extractor (described in further detail in Section D).

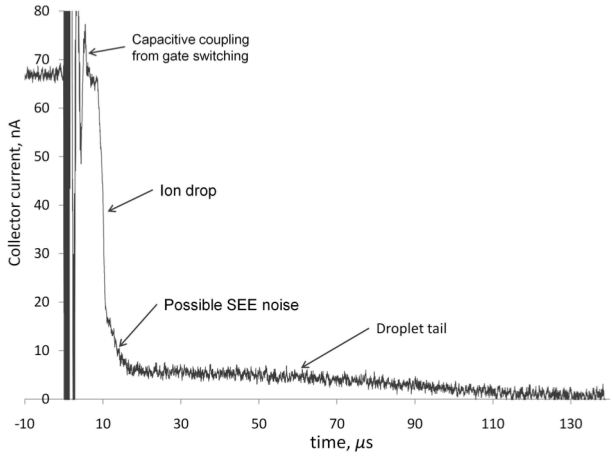

Figure 8. ToF curve for EMI-BF_4 using a 10 μ m emitter. In uni-polar mode, with an applied back pressure of 1.3×10^{-3} mBar (reservoir chamber fully evacuated).

The total current read on the collector is 65.5nA, compared to the emitter current of 780nA; hence approximately 8.5% of the current reached the collector 0.25m downstream. This percentage collected is fairly typical of the results.

The ToF trace indicates a mixed ion-droplet mode, with ions making up the majority of the spray (~91% of the current). The droplet tail is relatively long, indicating slow moving charged droplets. There is also some suggestion of secondary electron emission (SEE) occurring after the ions have collided with the collector. The species charge to mass ratio is related to the current drop by;

$$\left(\frac{q}{m}\right)_{i,d} = \frac{\left(L_{TOF}/t_{i,d}\right)^2}{2V_{em}} \qquad (1)$$

Where L_{TOF} is the distance between the ToF gate and the collector, V_{em} is the voltage accelerating the charged particles (assumed to be the applied emitter voltage as voltage losses are unknown at this point without testing the energy spread of the plume), and $t_{i,\,d}$ is the point at which the ion or droplet current falls away. For the ions this current drop off is quite abrupt, and therefore the ion q/m ratio can be estimated quite accurately. For the droplets the current tails off, a demonstration that there is a mix of droplet species involved, and the calculated charge to

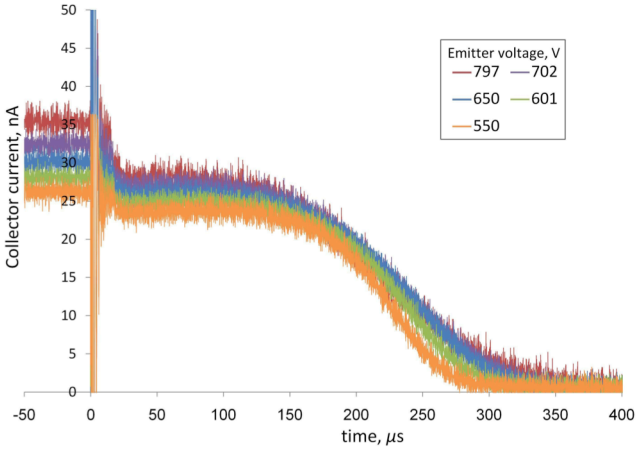

Figure 9. ToF curve for EMI-TF_2N using a 10 μ m emitter. In uni-polar mode, with an applied back pressure of 20 mBar (reservoir chamber fully evacuated).

mass ratio is going to be only approximate. Even so the respective q/m ratios can be estimated, with $(q/m)_i = 4.1\times10^5$ C/Kg, and $(q/m)_d = 4.1\times10^3$ C/Kg. Therefore there is a very large difference between the ion and droplet characteristics.

Figure 9 illustrates the variation of the ToF trace with emitter voltage, for EMI-TF_2N. The experiment was in unipolar mode, using again a 10μm inner diameter emitter, with a applied back pressure of 20 mBar. The emitter successfully sprayed from 550V to 800V. The ToF curves all demonstrate a spray dominated by droplets, with only a slight amount of ion current in evidence. The percentage of ion current varied from 9.2% to 20.3%, increasing slightly with applied voltage. The overall current also increased slightly with voltage, with on average ~10% of the emitter current collected.

There is a very significant difference between the EMI-BF_4 and EMI-TF_2N curves illustrated. This is more clearly demonstrated in Figure 10, where ToF traces for both are shown using 10µm inner diameter emitters, under similar conditions. There is some variation in applied voltage and back (reservoir) pressure but it is felt that these minor changes in conditions are not significant with regard to the changed ToF profiles observed. As well as the EMI-TF_2N trace being more droplet-biased, its droplet tail is longer. Using equation (1) the $(q/m)_d$ ~1×10^2 C/Kg, an order of magnitude smaller than that found for EMI-BF_4.

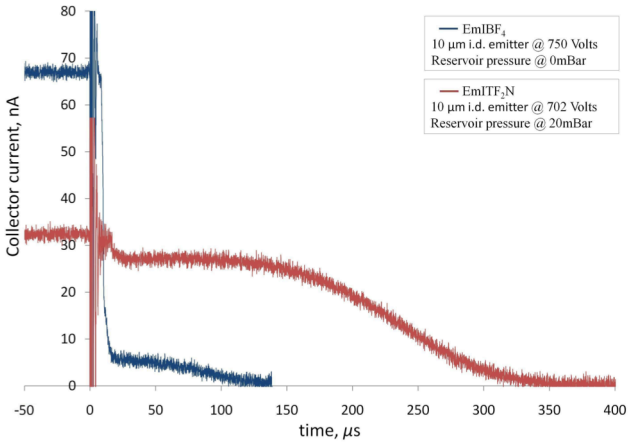

Figure 10. Comparison between EMI-BF_4 and EMI-TF_2N ToF curves under similar conditions.

A possible reason for EMI-TF_2N producing less ionic sprays is the lower surface tension and conductivity of the fluid compared to EMI-BF_4. This has been found to reduce the electric field at the cone-jet transition region[9], resulting in less ion emission from the meniscus.

From the ToF traces the specific impulse can be estimated using;

$$I_{sp} = \frac{L_{TOF}}{2\, g_0} \frac{\int_0^\infty i(t)\mathrm{d}t}{\int_0^\infty i(t)\; t\; \mathrm{d}t}, \tag{2}$$

where g_0 is earth's gravitational constant. For the typical EMI-BF_4 trace shown above I_{sp} = 461s. This compares to the theoretical maximum if only monomer cations are emitted of 3680s. For the EMI-TF_2N trace shown in Figure 10 the I_{sp} is of the order 50s; clearly too low for operational purposes. It is clear that working in a mixed ion-droplet regime is very detrimental to the I_{sp} of the spray; a conclusion that agrees with previous studies[10]. This detrimental performance is particularly evident when there is a large difference in the charge to mass ratio of the droplets compared to the ions. This is the case with EMI-TF_2N, as shown by the long droplet tail. For these 10µm emitters, and also for the 15µm emitters, it would seem that the hydraulic impedance was not high enough to reduce the flow rate to a point where the spray was ion-dominated. One obvious method to reduce the flow rate, given the thruster configuration, is to adopt a smaller inner diameter for the emitter.

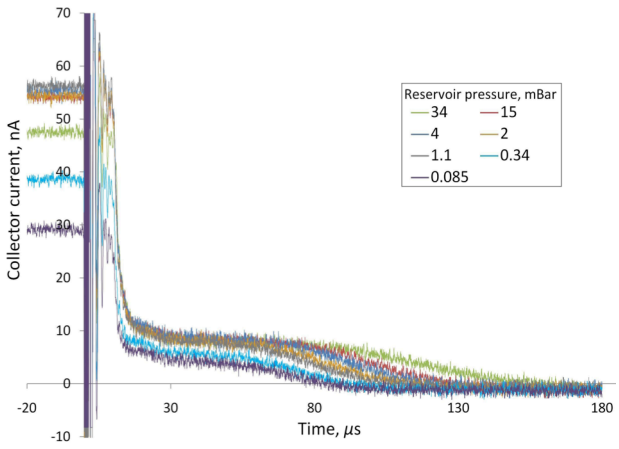

Figure 11. The variation of ToF curves with applied back pressure. Using EMI-BF_4, in uni-polar mode and with a 5 µm emitter.

To investigate this flow rate dependence ToF data was collected also for the 5 μm emitter, in unipolar mode, and with the propellant EMI-BF_4. A variation in back pressure was applied, resulting in ToF traces, as illustrated in Figure 11. The voltage applied to the emitter is 752V in all cases shown.

As the back pressure was decreased, the droplet tail on the ToF traces decreased in length; hence the droplet charge to mass ratio increased. Therefore there was less difference between $(q/m)_i$ and $(q/m)_d$.

The I_{sp} at different applied reservoir back pressures is shown in Figure 12. Results for three voltages are illustrated; 700, 752, and 806V. At 752V, as would be expected from the ToF curves in Figure 11, the specific impulse increases as the back pressure is reduced. The same is true for 700V where the specific impulse approaches 2000s, with a back pressure of 4 mBar.

The voltage applied also has a noticeable effect on the performance; at higher applied voltages reducing the reservoir back pressure has less effect on the specific impulse. This effect may be an artifact of the fact that as the voltage is increased, the flow rate from an electrospray emitter has been found to increase (an effect that may be large for such a small emitter)[11,12]. Hence with the larger emitter flow rate at higher voltages, the ionic regime cannot be reached, and the I_{sp} is small. With 806V applied to the emitter, even at low reservoir pressures the electrospray was in a mixed ion-droplet regime.

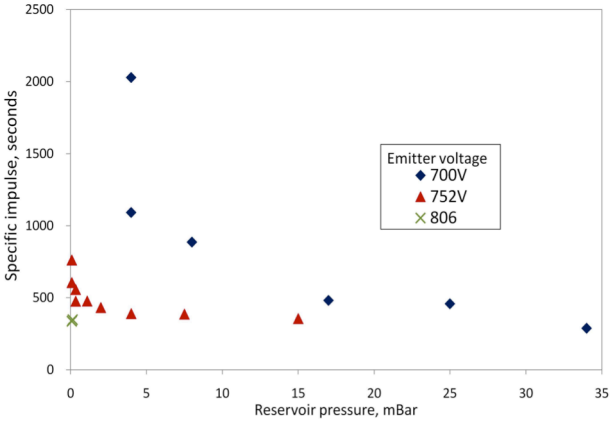

Figure 12. Variation of I_{sp} with reservoir back pressure. Using EMI-BF4, in uni-polar mode, and with a 5μm emitter.

D. Failure modes

Although successful sprays were completed using various different sized emitters, controlling the liquid wetting of the emitter was difficult. This was especially true of the 10 and 15 μm inner diameter emitters, where in uni-polar mode, and with a reservoir pressure applying a flow rate, it was difficult to avoid the wetting of the ionic liquid between the emitter and extractor. An indication of the difficulties involved can be seen in the pressure needed to be applied to initiate spraying. For the 5µm emitter this initialization back pressure was 120 mbar, whilst for the previously tested silica microsphere-filled emitters[7] it varied from 180 to 500 mBar; this variation in backing pressure onset is likely to be dependent upon the filling factor of the microspheres, a reason indeed to move to the new configuration reported here. For the 10 and 15µm emitters the initiation back pressure was of the order 10 - 40mBar, a pressure which proved difficult to operate at without the liquid wetting between the emitter and extractor. This was in part due to the operational difficulty of accurately acquiring a pressure at this small pressure difference, but mostly it seemed that with the relatively low hydraulic impedance of the 10 and 15µm emitters (the impedance of the 10µm emitter is an order of magnitude smaller than the 5µm emitter), the fluid could be much more easily extracted by the voltage from the emitter. Indeed the voltage extraction of fluid in an electrospray emitter has been found to be dependent on hydraulic impedance [3, 4]. Hence too much fluid was extracted for a Taylor cone to form, and instead it seemed that the fluid wetted the 50µm distance between the emitter tip and the extractor.

V. Ionic Liquid Wetting

A. Filling by capillary action

Controlling the propellant transport in the thruster system requires a very good understanding of its wetting properties. In the absence of gravity, filling of the emitters can be entirely assessed through the contact angle of the liquid with a given surface. Because of its simplicity, the sessile drop method was chosen to measure the contact angles of two candidate ionic liquids (EMI – BF_4 and EMI – TF_2N, purchased from IoLiTec[8]) on several

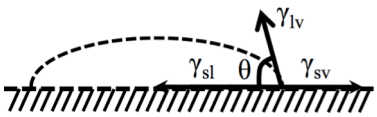

Figure 13. Diagram of interfacial tensions defining the contact angle of a drop.

[8] IoLiTec Ionic Liquids Technologies GmbH Salzstrasse, Germany (http://www.iolitec.de/)

surfaces which could be used either as material in the upstream liquid delivery system or to coat the chip itself. This method consists of dropping small amounts of liquid on a substrate and measuring the angle θ at the edge of the drop, as shown in Figure 13. This angle is then related to γ_{sv}, γ_{sl}, and γ_{lv}, respectively the solid-vapor, solid-liquid and liquid-vapor (commonly referred to as the surface tension of a liquid) interfacial tensions according to equation (1).

$$\cos(\theta) = \frac{\gamma_{sv} - \gamma_{sl}}{\gamma_{lv}} \qquad (4)$$

B. Measurement setup

To avoid reported[13] contamination by ambient humidity, the experiment was performed in vacuum (below 10^{-5} mbar). The IL was kept in a secondary vacuum chamber with a submersed 150 µm glass capillary. IL was transferred to the primary chamber and the substrates by pressurizing the secondary chamber with nitrogen. The substrates were placed on a linear motion mechanical feed-through, allowing several drops to be placed alongside on a given substrate and/or several substrates within a test sequence (Figure 14). At the beginning of each test sequence, the transfer capillary was flushed for at least 30 minutes in a reservoir to eliminate all liquid in the capillary when the main chamber was vented. Drops were then placed (falling by their own weight) on the samples with a USB camera imaging from within the chamber. Snapshots from the videos were then analyzed with the ImageJ[9] open source software using the DropSnake[14] plugin. Substrate temperature was controlled using a thermoelectric module (TE1-19908L) in closed feedback with a Pt1000 temperature probe. It remained at approximately 30 °C for "ambient" tests and was increased to 80 °C for high temperature tests. The two candidate ionic liquids, EMI-BF_4 and EMI-TF_2N were studied on 11 surfaces: polished silicon, silicon dioxide, silicon nitride, gold, platinum, aluminum, glass, Teflon and three layers deposited by Molecular Vapor Deposition[10] (MVD A, B, C). MVD A silane-based coating showed lowest surface energy. MVD C metal-oxide based coating showed the highest surface energy values among MVD A,B and C coatings. All measurements were then retaken on the vented chamber, after at least one hour of exposition to ambient air.

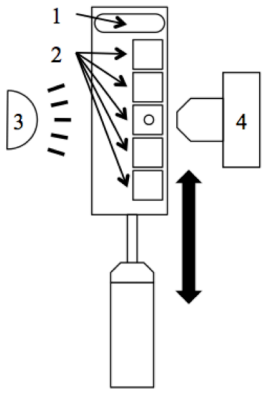

Figure 14. Top view of drop application setup. 1) Dispense reservoir, 2) Test substrates, 3) Light source, 4) USB camera

C. Contact angle results

Results of average contact angle in vacuum at room temperature are shown in Figure 15. EMI – BF_4, with its higher reported surface tension (44.3 dyn/cm @ 22-25°C)[13], has larger contact angles with all surfaces tested than EMI – TF_2N (35.2 dyn/cm @ 22-25°C)[13]. Two surfaces, polished silicon and *MVD A*, exhibited contact angles larger than 90°, making them good candidates as surfaces which should not be

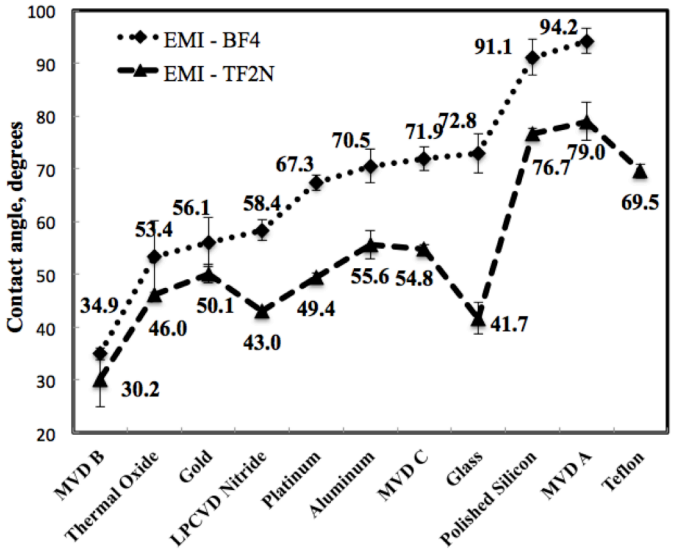

Figure 15. Average contact angle of EMI – BF_4 and EMI – TF_2N on several substrates, in vacuum at room temperature.

[9] Available for download http://rsbweb.nih.gov/ij/

[10] Molecular Vapor Deposition (MVD) is a technique for the deposition of ultra-thin molecular layers from the gas phase precursor. The deposited layers are predominantly organic or organometallic in nature and are controlled on a molecular level at ambient temperature.

wetted. The "hydrophobic"[11] MVD layer in particular could be coated on the emitter, provided adequate protection of its interior and reduce the occurrence of liquid overflow failures described earlier. None of the surfaces tested with EMI – TF_2N exhibited larger than 90° contact angles. The surfaces also did not exhibit any significant dependence on substrate temperature (results for EMI – BF_4 are shown in Figure 16), a positive element from the system perspective. Finally, neither of the ionic liquids showed significant variations when subjected to air for over one hour (Figure 17), despite evidence of water uptake of EMI-BF_4 as reported by Martino et al.[13] This difference may indeed be due to the experimental setup. They used the capillary rise method with a small glass capillary (273µm radius) and measured a contact angle of 5.7° (= *cos 0.995*[13] for EMI-BF_4). Ambient humidity may then have more easily penetrated the very thin film of liquid and had a rapid effect on the angle. In our case, it is speculated that either the exposure time was too short to measure any significant difference or that the water absorption also acted on the liquid-solid interfacial tension, counterbalancing a change in liquid-gas interfacial tension.

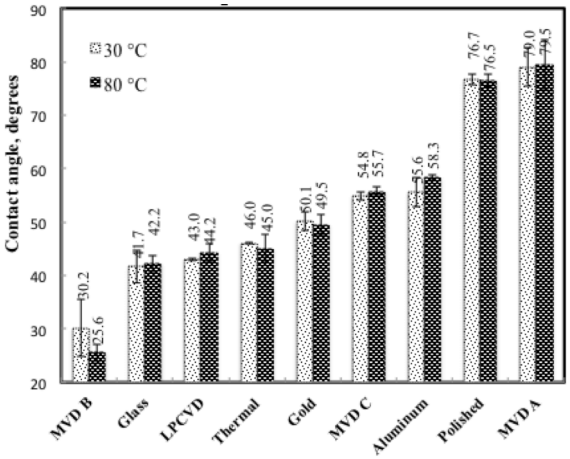

Figure 16. Average contact angle of EMI – TF_2N on several substrates, in vacuum

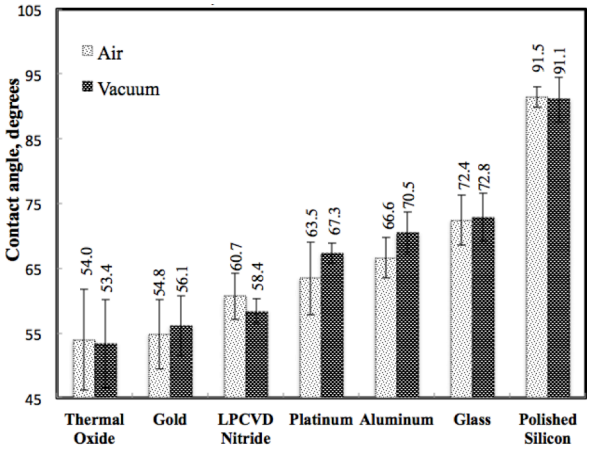

Figure 17. Average contact angle of EMI – BF_4 on several substrates, at 30 °C.

VI. Conclusion

We have presented a novel wafer-scale microfabrication process for integrated MEMS colloid thruster chips, with a density of 1600 emitters/cm^2. By bonding the extractor electrode wafer directly to the capillary "emitter" wafer, the assembly is greatly simplified compared to our earlier generation of devices, leading to higher yield and increased flexibility in array size. Wetting of different materials by ionic liquids must be mastered to guide the liquid where desired (capillary pumping) and to avoid lifetime-limiting liquid bridges. To aid in selecting the optimal materials for different ionic liquids, contact angle measurements were made for EMI-BF_4 and EMI-Tf_2N on a variety of materials, with the surprising observation that contact angle is unchanged upon heating from 30°C to 80°C.

We focus in this paper on data from single emitters. Mixed ion-droplet mode (>90% ion) was observed for the 10 µm ID capillaries for EMI-BF_4 with stable spraying seen down to 500V. For EMI-Tf_2N under similar conditions, only 10% of the beam consisted of ions. The 5µm ID capillaries have higher hydraulic impedance, making it easier to reach the pure ion regime, associated in our geometry with very low flow rates. With 700 V applied between emitter and extractor, a specific impulse of 2000 s was determined from TOF data for a 5 µm capillary filled with EMI-BF_4.

This work is an important step towards the development of MEMS thruster chips that will be integrated into a complete miniaturized EP thruster system being developed by a European consortium in the framework of the EU FP7 project MicroThrust.

[11] The term hydrophobic is used here for simplicity, although it refers to the wetting properties of water specifically

Acknowledgments

This work has been supported by the MicroThrust project, grant agreement number 263035, funded by the EC Seventh Framework Programme theme FP7-SPACE-2010 (www.microthrust.net). S. D. thanks Olga Fryckova of CSEM for advice and providing the MVD samples as well as Nicolas Blondiaux for help and training on the CSEM goniometer.

References

[1]Taylor, G. "Disintegration of water drops in an electric field." *Proceedings of the Royal Society* of 280, no. 1382 (July 1964): 383-397.

[2]Romero-Sanz, I., R. Bocanegra, J. Fernandez de la Mora, and M. Gamero-Castaño. "Source of heavy molecular ions based on Taylor cones of ionic liquids operating in the pure ion evaporation regime." *Journal of Applied Physics* 94, no. 5 (2003)

[3]Lozano, Paulo C., and Manuel Martínez-Sánchez. "Ionic liquid ion sources: characterization of externally wetted emitters." *Journal of Colloid and Interface Science* 282, no. 2 (February 2005): 415-21.

[4]Legge, Robert S., and Paulo C. Lozano. "Electrospray Propulsion Based on Emitters Microfabricated in Porous Metals." *Journal of Propulsion and Power* 27, no. 2 (March 2011): 485-495.

[5]Courtney, DG, and P. Lozano. "Development of Ionic Liquid Electrospray Thrusters using Porous Emitter Substrates." In *International Conference on Space Technology and Science*, 1-6, 2009.

[6]Krpoun, Renato, M. Räber, and Hebert R. Shea. "Microfabrication and test of an integrated colloid thruster." In *21st International Conference on Micro Electro Mechanical Systems*, 964-967, 2008.

[7]Krpoun, Renato, H. R. Shea. "Integrated out-of-plane nanoelectrospray thruster arrays for spacecraft propulsion." *Journal of Micromechanics and Microengineering* 19, no. 4 (April 2009): 045019.

[8]Krpoun, Renato, Katharine Lucy Smith, John P. W. Stark, and H. R. Shea. "Tailoring the hydraulic impedance of out-of-plane micromachined electrospray sources with integrated electrodes." *Applied Physics Letters* 94, no. 16 (2009): 163502.

[9]Gamero-Castaño, Manuel, and Juan Fernandez De La Mora. "Direct measurement of ion evaporation kinetics from electrified liquid surfaces." *The Journal of Chemical Physics* 113, no. 2 (2000)

[10]Lozano, Paulo C., and Manuel Martínez-Sánchez. "Studies on the ion-droplet mixed regime in colloid thrusters", PhD, MIT, 2003.

[11]Ryan, C N, K L Smith, M S Alexander, and J P W Stark. "Effect of emitter geometry on flow rate sensitivity to voltage in cone jet mode electrospray." *Journal of Physics D: Applied Physics* 42, no. 15 (August 7, 2009)

[12]Smith, Katharine L., Matthew S. Alexander, and John P. W. Stark. "The sensitivity of volumetric flow rate to applied voltage in cone-jet mode electrospray and the influence of solution properties and emitter geometry." *Physics of Fluids* 18, no. 9 (2006)

[13]Martino, W., Juan Fernandez De La Mora, Y. Yoshida, G. Saito, and J. "Surface tension measurements of highly conducting ionic liquids." *Green Chemistry* 8, no. 4 (2006): 390

[14]A.F. Stalder, G. Kulik, D. Sage, L. Barbieri, P. Hoffmann, "A Snake-Based Approach to Accurate Determination of Both Contact Points and Contact Angles", *Colloids And Surfaces A: Physicochemical And Engineering Aspects,* Vol. 286, No. 1-3, pp. 92-103, September 2006.